Annals of Anatomy 234 (2021) 151616

Contents lists available at ScienceDirect

Annals of Anatomy

journal homepage: www.elsevier.com/locate/aanat

Clinico-anatomical classification of the *processus condylaris mandibulae* for traumatological purposes

Bartosz Bielecki-Kowalski [a,*], Marcin Kozakiewicz [b]

[a] Department of Maxillofacial Surgery, Medical University of Lodz, 1st Gen. J. Haller Plaza, Lodz, Poland
[b] Department of Maxillofacial Surgery, Medical University of Lodz, 1st Gen. J. Haller Plaza, Lodz, Poland

ARTICLE INFO

Article history:
Received 20 September 2019
Received in revised form 4 September 2020
Accepted 25 September 2020

Keywords:
Mandible condyle
Morphological classification
Fracture treatment

ABSTRACT

Mandible condyle fracture has been reported to constitute 9–45 % (Asprino and Consani, 2006), 14.1 % (Bataineh, 1998), 25–50 % (Silvennoinen, Iizuka, 1992), 32 % (Chrcanovic et al., 2004), and 38 % (Brasileiro and Passeri, 2006) of all mandible fractures (Kozakiewicz and Swiniarski, 2013). Small bone segments, limited available space for application of the fixation material and limited visibility of the operative field are common difficulties. To guarantee satisfactory treatment effects, anatomical reduction and proper fracture stability are necessary. The use of 3–4 screws in the upper section (proximal segment) provides adequate immobilization, which can be easily achieved when the condyle is low and wide. However, if the condyle is slender, it is not technically possible to fix 2 plates and 4 screws for osteosynthesis. Selection of the appropriate fixative material that will provide adequate rigidity during the healing period while simultaneously allowing proper construction of the lateral silhouette of the processus condylaris mandibulae to fix the plate remains a key consideration.

The aim of this study was to evaluate clinico-anatomical classification of the condyle of mandible posture for traumatological purposes. Five hundred computer tomography virtual models were created, from which 11 measurements were made, and 2 indexes were calculated. Assessment of types based on the ratio of the condyle height index revealed a dichotomous division into high and short condyles. Statistically associated with the division, the Width_neck_basal (the width of the bone at the level of semilunar notch measured by a frontal projection perpendicular to line "A", as described by Neff (Neff et al., 2014)) measurement allowed the creation of the following clinico-anatomical classification: -slender-type condyles have a Width_neck_basal in the range of 4–8.5 mm; -squad-type condyles have a Width_neck_basal in the range of 11.5–19.5 mm.

Patients with a Width_neck_basal value in the 8.5–11.5 mm range cannot be classified using this method, and a different method to assess the lateral condylar silhouette must be used. The proposed clinic-anatomical classification method avoids the problems associated with incorrect osteosynthesis plate selection. Assignment to a group can be obtained by making one measurement (the Width_neck_basal). In that way, the optimal fixing material can be selected by the surgeon before the operation commences, with great intraoperation time savings.

1. Introduction

Mandible condylar fracture is the most frequent mandible fracture in humans and the major challenge in maxillofacial traumatology. Epidemiologically, mandible condylar fracture constitutes 9–45 % (Asprino and Consani, 2006), 14.1 % (Bataineh, 1998), 25–50 %(Silvennoinen and Iizuka, 1992), 32 % (Chrcanovic et al., 2004), and 38 % (Brasileiro and Passeri, 2006) of all mandible fractures (Kozakiewicz and Swiniarski, 2013). The mainstay of condylar fracture treatment is open reduction and internal fixation (ORIF). ORIF allows us to obtain statistically better outcomes in the treatment of displaced and dislocated fractures among maxillofacial fractures (Korzon and Kruk, 1971; Cascone et al., 2008) and restores preinjury dental occlusion (Brin et al., 2012). The main issue is the difficult surgical approach, which requires facial nerve branch preparation and operation in a small treatment field, which increase the risk of postoperative facial nerve palsy and extraoral salivary fistula. Various authors have reported that the first complication occurs in 8.6–55 % (Ellis et al., 2009), 12.5 % (Bruneau et al.,

* Corresponding author.
E-mail addresses: bartoszkowalski@gmail.com (B. Bielecki-Kowalski), marcin.kozakiewicz@umed.lodz.pl (M. Kozakiewicz).

https://doi.org/10.1016/j.aanat.2020.151616
0940-9602/

2018) or 17.2 % (Ellis et al., 2000) of patients treated with ORIF, but permanent paresis is a concern, depending on the approach, in only 0.3 %, 1.4 %, 1.5 % or 2.2 % of patients(Al-Moraissi et al., 2018). Extraoral salivary fistula occurs in 2.3 % of patients and can be treated surgically (Bhutia et al., 2013). Unfortunately, other challenges remain. Small bone segments, limited available space for application of the fixation material, limited visibility of the operative field, and the high force exerted on the fixed fractures require proper preoperational anatomical reconnaissance for the best choice of the efficient fixative material.

To guarantee satisfactory treatment effects, anatomical reduction and proper fracture stability are necessary. The standard is using two osteosynthesis plates that are fastened divergently and fixed with four screws in the proximal (upper) segment. This procedure is easy to complete when the condyle is wide and short, but it can be difficult to achieve and even impossible for more narrow and slender condyle processes. Many plates are available for osteosynthesis of the processus condylaris mandibulae, but only four of them are dedicated to stabilizing slender condyles. On the other hand, these plates should not be used to stabilize wide, short condyles due to the divergent vectors of stress distribution in the bone (Meyer et al., 2002). The above issues motivated the search for a method that would allow the classification of condyles in terms of considerations for selecting the proper plates.

The aim of this study was to develop a clinico-anatomical classification system of the condyle of mandible posture for traumatological purposes.

2. Material and methods

2.1. Experimental design

Approval for this study was obtained under bioethics committee numbers RNN/125/15/KE and RNN/738/12/KB. Five hundred condyles were examined by computed tomography (CT)-based three-dimensional models of Caucasian subjects aged 18–88 years. Datasets were obtained from both sides of the mandible from cone beam computed tomography (CBCT) using Carestream CS 9300 3D software (Carestream Dental LLC, Atlanta, GA, USA) and from spiral fan beam computed tomography (FBCT) using a 320-MDCT volumetric scanner (Aquilion ONE, Toshiba, Otawara, Japan). Sixty-six CBCT and 184 FBCT images of the mandible (two condyles from each CT) were acquired after anonymization of patients (Newhauser et al., 2014) from the Maxillofacial Surgery Department Database.

The inclusion criteria were an intact processus condylaris of the mandible and whole rest of the mandible visible on CT. The exclusion criteria were as follows: premature age of the scanned patient, patients affected by degenerative lesions of the temporomandibular joint region (e.g., ankylosis, malignancy, fibrous dysplasia), posttraumatic region of the mandible, after ORIF and after resection treatment of the mandible, low quality tomographies and numerous artifacts in the image.

DICOM axial image series were transformed into 3D models of bone using segmentation. Bone segmentation was performed using global thresholding defined for CBCT and FBCT by individual histogram analysis according to the Baillard and Barillot protocol (Baillard and Barillot, 2000). Subsequently, the obtained models were subjected to measurements. Segmentation, model preparation and measurements were performed in Mimics 17.0 software (Materialise, Leuven, Belgium).

For all models, auxiliary line “A” was determined by the algorithm described by Neff (Neff et al., 2014). The mandible model was placed in 3D space with auxiliary line A positioned parallel to the Y axis. All measurements described below (Fig. 1) were applied to the models perpendicularly to line “A”:

1 Length_neck_basal- the distance between the lowest point in the semilunar notch of the mandible and the back-most point of the ramus at that level;
2 Length_neck_top- the distance between the forward-most and back-most points at the level of the condylar head reference line, as described by Neff (Neff et al., 2014);
3 Distance_sigmoid notch-neck top- the distance between the forward-most points of the two lines described above;
4 Height_neck- the distance between Length_neck_basal and Length_neck_top measured parallelly to line “A”;
5 Length_neck_middle- the distance between the forward-most and back-most point at the level of ½ of the Height_neck;
6 Ramus height- the height of the ramus of the mandible measured parallel to line “A” and crossing the highest point of the head of the mandible.

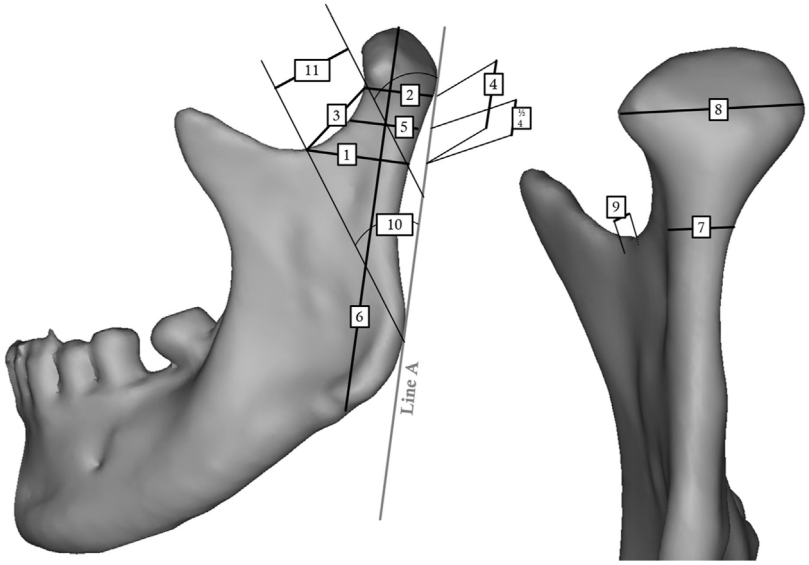

Fig. 1. Measurements: Length_neck_basal (1), Length_neck_top (2), Distance_sigmoid notch-neck top (3), Height_neck (4), Length_neck_middle (5), Ramus height (6), Width_neck_basal (7), Width_head (8), Thickness_sigmoid_notch (9), Angle_posterior line-notch point (10), Height_neck_new_classification (11) and line “A”, which is tangential to the posterior border of the ramus of the mandible.

Three diameters perpendicular to line "A" were measured in the frontal projection:

7 Width_neck_basal- the width between medial-most and lateral-most point at the level of Length_neck_basal;
8 Width_head- the widest measurement of the head of the mandible;
9 Thickness_sigmoid_notch- the width measured 1 mm below the sigmoid notch- the point is significant due to medial ramus of A-shape osteosynthesis plate stabilized by bicortical screw in sigmoid notch area- followed by cortical bone evaluation(Rajchel et al., 1986);
10 Angle_posterior line-notch point- the angle between the line running through the lowest point in the semilunar notch and the lowest point on line "A" tangential to the ramus and "A" line itself;
11 Height_neck_new_classification (Kozakiewicz, 2019)- the distance between the medial arms of the corresponding angle for which one arm is the line andCHI the second arm is defined by the forward-most points of Length_neck_basal and Length_neck_top.

The condyle height index (CHI) and the condyle slenderness index (CSI) were calculated as second-order anatomical features for all investigated processus condylaris of the mandible. CHI combines Length_neck_basal with Height_neck measurements according to the following equation:

$$CHI = \sqrt{\frac{Height\_neck}{Length\_neck\_basal}}$$

The square root normalizes the distribution. In turn, CSI combines Length_neck_top and Height_neck calculated from the following equation:

$$CSI = \frac{14}{13} + \log_{10}\frac{Height\_neck}{Length\_neck\_top}$$

The factor normalizes the average CSI to 1.0, and the logarithm normalizes the distribution.

2.2. Statistical analysis

For all condyle measurements (Fig. 1), including CHI and CSI, summary statistics were calculated to obtain the separation between groups of patients according to the type of condyle. ANOVA for CSI was performed to determine whether CSI, which better describes the lateral silhouette of the condylar process, is correlated with the CHI-based dichotomic division. To determine whether CSI depends on the patient's sex or age, one-way analysis of variance and linear regression were performed.

All measurements (Length_neck_basal, Length_neck_top, Distance_sigmoid notch-neck top, Height_neck, Length_neck_middle, Ramus height, Width_neck_basal, Width_head, Thickness_sigmoid_notch, Angle_posterior line-notch point, Height_neck_new_classification) and indexes (CHI and CSI) were investigated by factor analysis. Horizontal factors, vertical factors, and sagittal factors were extracted. These factors and CHI were analyzed using a Bayesian artificial neural network for all condyles to predict the lateral silhouette of the condylar process.

To obtain a measurement unbound with Height_neck measurement and strongly associated with anatomical classification into slender and squat condyles, measurements of the condyle base were subjected to regression analysis.

Because CSI is dependent on Width_neck_basal, which allows the maintenance of CSI-based dichotomic division, condylar slenderness was categorized based only on the condylar base thickness measurement (Width_neck_basal) using discriminant analysis. All cases were used to develop a model to discriminate between the two levels of CSI divided categorically (a CSI value equal to 1.0 was set as the threshold to divide the categories). Using this procedure, slender-type and squad-type of processus condylaris mandibulae could be differentiated.

The standard deviation was added to the average value of Width_neck_basal in the slender-type condyle group to determine how close the diameters are to those of the squat-type condyle group. The standard deviation was subtracted from the average Width_neck_basal of the squad-type condyle group to determine how close the value is to that of the slender-type condyle group.

Table 1
Summary statistics of the radiological anatomy of the processus condylaris mandibulae.

Measure/calculation	Average ± SD	Minimum	Maximum
Length_neck_basal	20.9 ± 2.6 mm	13.5mm	27.3mm
Lenght_neck_middle	13.0 ± 1.9 mm	7.0mm	22.1mm
Length_neck_top	11.8 ± 1.7 mm	6.6mm	17.3mm
Distance_sigmoid notch-neck top	14.7 ± 3.1 mm	7.2mm	25.1mm
Height_neck	10.2 ± 2.7 mm	4.0mm	20.7mm
Width_neck_basal	10.0 ± 3.0 mm	4.0mm	19.6mm
Width_head	20.5 ± 2.5 mm	11.1mm	27.9mm
Thickness_sigmoid_notch	2.0 ± 0.8 mm	0.8mm	5.6mm
Ramus height	68.8 ± 6.0 mm	51.7mm	89.0mm
Condyle angulation	37.0° ± 18.8°	0.3°	90.0°
Height_neck_new_classification	14.4 ± 2.9 mm	8.0mm	23.7mm
Angle_posterior line-notch point	38.0° ± 4.6°	21.3°	53.2°
Condyle height index (CHI)	0.697 ± 0.092	0.387	0.960
Condyle slenderness index (CSI)	1.0 ± 0.135	0.135	0.554

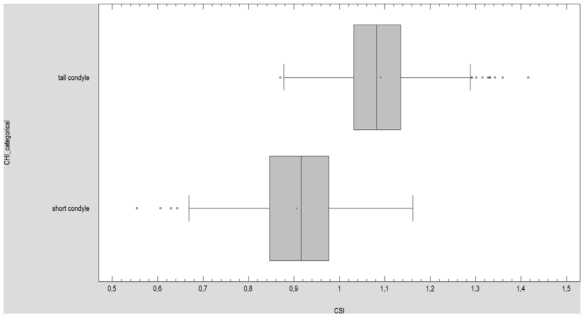

Fig. 2. Evaluation of the processus condylaris types based on CHI. This index is based on the relation of height to length, and likewise, the category names are reflective of tall and short condyles. The point of dichotomic division according to the CSI value is near 1.0, consistent with the assessment of the height of condyles based on CHI ($p < 0.001$).

3. Results

The average age of patients included in the CT evaluation was 44.6 ± 18 years. Summary statistics revealed an average CSI value of 1.0 and a CHI value of 0.697 (Table 1). These values were set as division points for dichotomous division. In the case of CSI, the division threshold for condyles was 1: CSI ≤ 1 for the squat type and CSI > 1 for the slender type. CHI indicates a short condyle when CHI is less than or equal to 0.697. Condyles with CHI greater than 0.697 were classified as tall.

Condyles were dichotomously divided into categories based on CHI, i.e., slender condyles and squat condyles (Fig. 2), whereas the combination of the two indices allowed for further satisfactory separation of the condyles based on CSI. ANOVA with the CHI-based factor presented a strong separation of the two morphological types characterized by CSI values ($F = 447$, $p < 0.0001$). As CSI better describes the lateral silhouette of the condylar process, further statistical analysis was conducted.

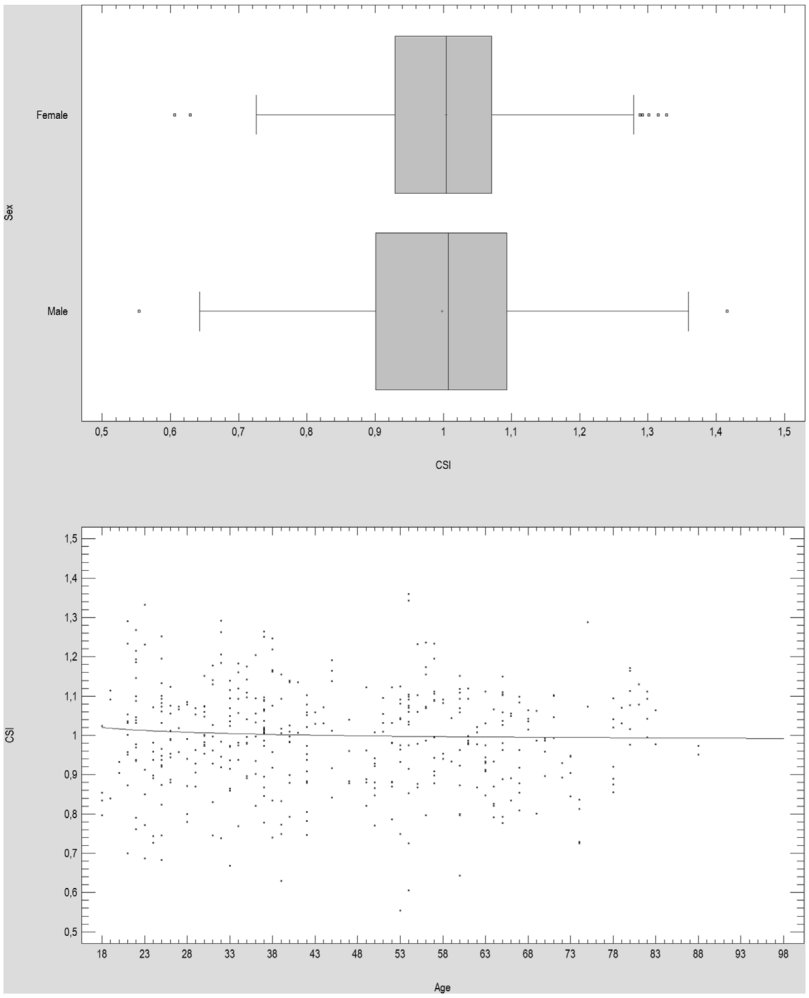

Fig. 3. Dependence of CSI on sex and age. No significant differences were found ($p > 0.05$). CSI is sex- and age-independent.

Table 2
Factor loading matrix after varimax rotation.

	Vertical Factor	Sagittal Factor	Horizontal Factor	Estimated Communality	Specific Variance
Length_neck_basal	026	085	004	079	021
Length_neck_top	−0,15	072	028	062	038
Length_neck_middle	−0,14	088	014	082	018
Width_neck_basal	−0,32	003	078	071	029
Width_head	−0,04	035	079	074	025
Height_neck	096	011	−0,13	094	005
Height_neck_new_classification	078	034	−0,09	074	026
Condyle Height Index (CHI)	087	−0,28	−0,15	086	014
Condyle Slenderness Index (CSI)	092	−0,23	−0,24	096	004

ANOVA and linear regression revealed that CSI could be used as a universal factor independent of the age and sex of the patient (Fig. 3).

Length_neck_basal, Length_neck_top, Length_neck_middle, Width_neck_basal, Width_head, Height_neck, Height_neck_new_classification, CHI and CSI included in the factor analysis allowed for extraction of three strong factors that explain the variability resulting from all nine included variables. These three factors were Horizontal_Factor, Vertical_Factor and Sagittal_Factor (Table 2, Fig. 4).

The effectiveness of the classification as a slender- or squat-type processus condylaris was verified by neural network analysis (Fig. 5). A very high level of correct predictions was obtained for the dichotomic classification into slender or squat processus. The percentage of cases correctly classified was 91.7 %.

Polynomial regression (Fig. 6) revealed that the Width_neck_basal of the bone in the area of the base of the condylar process is inversely related to the CSI. Thinner bone at the base of the condylar process corresponds to a more slender condylar process ($p < 0.001$).

Discriminant analysis of condylar slenderness, categorized based on the Width_neck_basal discriminated function with a p-value less than 0.05, corresponding to significance at the 95.0 % confidence level. Among the 500 observations used to fit the model, 358 were correctly classified. Radiological separation of both types in CT images was possible for 71.6 % of patients.

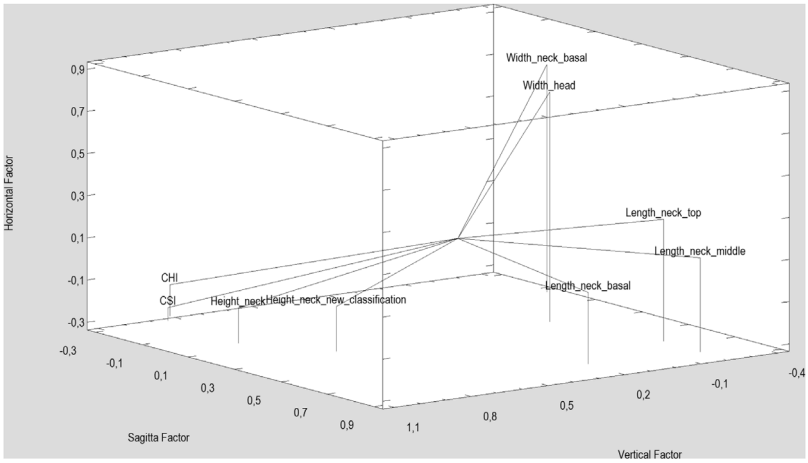

Fig. 4. Factor loadings. Varimax rotation of the matrix was performed to simplify the explanations of the factors. Raw variables are grouped into three factors.

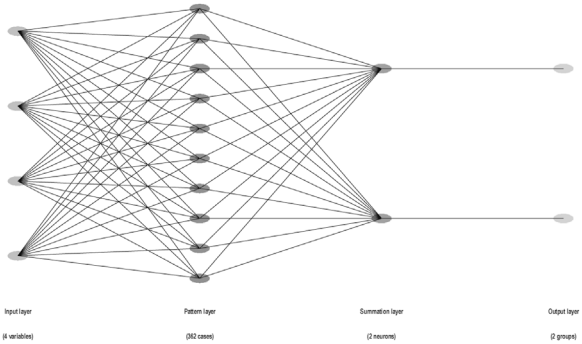

Fig. 5. Neural network Bayesian classifier for the prediction of the type of mandibular condylar process based on the following input factors for enhancing the classification power: vertical factor, sagittal factor, horizontal factor, and CHI (the above categorical classification results are defined based on CSI). Output: slender-type or squat-type processus.

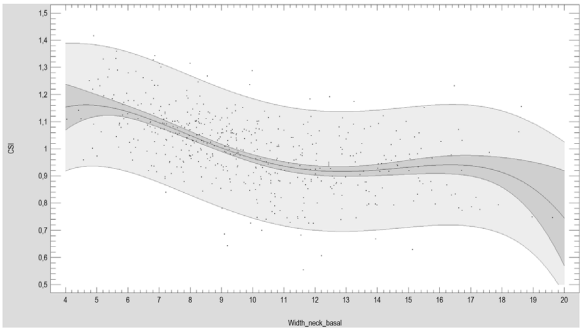

Fig. 6. The relation of CSI with the width of the base of the processus condylaris mandibulae. The output shows the results of fitting a fourth-order polynomial model to describe the relationship. Since the p-value according to ANOVA is less than 0.05, CSI and Width_neck_basal have a significant relationship.
Light gray – prediction limits; dark gray area – confidence limits at the 95 % confidence level.

Adding the standard deviation to the average Width_neck_basal of slender-type condyles and subtracting the standard deviation from the average Width_neck_basal of squat-type condyles, an intermediate category defined as a mixed morphological condylar process types can be described. Patients with Width_neck_basal in the 8.5–11.5 mm range belong to this category. Thus, the obtained results led to the development of the following clinico-anatomical classification:

-slender-type condyles have a Width_neck_basal in the range of 4–8.5 mm;

-squat-type condyles have a Width_neck_basal in the range of 11.5–19.5 mm.

4. Discussion

Several anatomical classifications of condyles were established. Yale's classification, even modified by Juniper (1994) and Yale et al. (1963), is not relevant to the most frequent condylar process fractures because head condylar fractures are rare. Unfortunately, these classification systems do not take into account the practical aspect of condylar osteosynthesis, and there, that their use in hospital practice is negligible.

Among the methods used for condylar fracture fixation, some intraoperative and postoperative complications have been indicated (Wagner et al., 2002). The most important for proper plate fixation is the lateral silhouette of the processus condylaris. Most postoperative complications are a result of insufficient stability of fixed bone segments, which is a main factor responsible for incorrect bone healing. The standard method of treatment aims to achieve osteosynthesis with two plates arranged along the line of propagation of bone stresses, i.e., diverging downwards. The use of 3–4 screws in the upper section (proximal segment) provides adequate immobilization (Aquilina et al., 2013; Kozakiewicz and Swiniarski, 2013; Kozakiewicz and Świniarski, 2017), which is easy to achieve when the condyle is short and wide. However, if the anatomy of the condyle is slender, it is not technically possible to fix two plates and four upper screws for osteosynthesis; this limitation may be frustrating intraoperationally in operating theatre. A critical consideration is the selection of the most appropriate fixation material to provide adequate strength during the healing period that simultaneously has the proper construction for the lateral silhouette of the processus condylaris mandibulae to fix the plate. This is an extremely important aspect for patients in the postsurgical period because the restoration of joint function should be rapid and can often occur as early as the first day after surgery.

The solution to the abovementioned problem may be the classification of condyles based on anatomical guidelines (measurements) with the aim of selecting the optimal fixation material.

For the first proposed method of estimating the lateral silhouette of the condylar process, the authors obtained a very high rate of correct predictions of the classification condyle shape; however, due to a number of factors (the height of the processus condylaris cannot be measured when the condyle is fractured), the surgeon can lose information related to condyle height. It is a result of

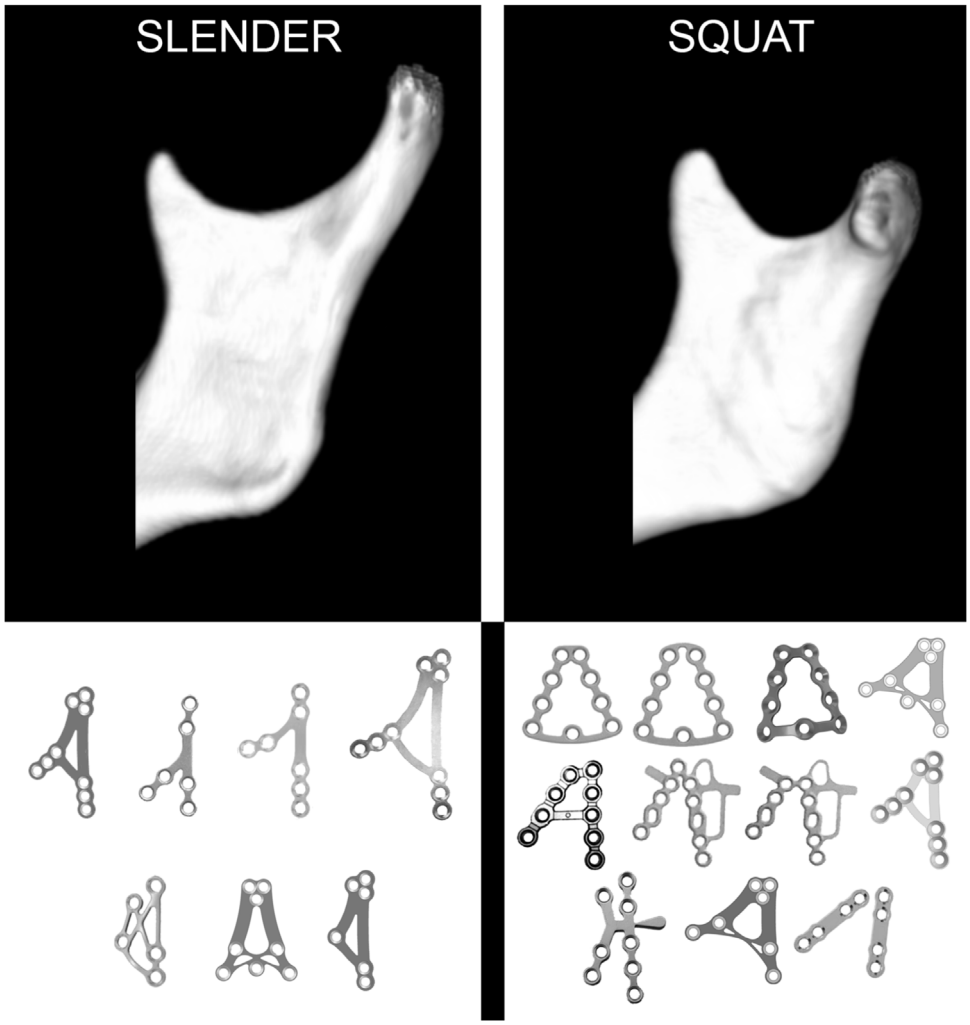

Fig. 7. Statistically supported clinico-anatomical classification of the condylar process of the mandible. A slender-type or squat-type diagnosis can lead to the proper choice of fixation material: The narrowed plates at the superior part are dedicated to slender-type condyles (left side), in contrast to wide plates, which are better fitted for osteosynthesis of squat-type mandibular condyles (right side).

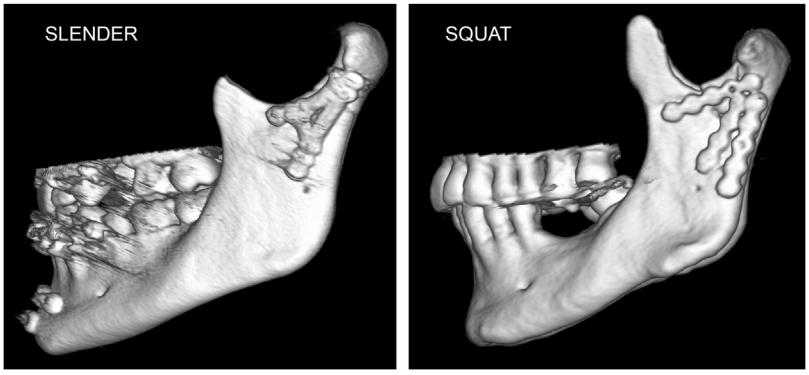

Fig. 8. An example of proper selection of platelets for osteosynthesis based on the anatomical variant of the condyle.

bone disruptor and segment displacement after fracture. Thus, this method should be applied to unilateral fractures only. However, this limitation represents the main weakness of our method because if there is an intact side then there is no need to perform numerous measurements. Evaluation of the intact condyle shape and selection of the proper fixation material is the solution.

A second important issue is how to assess belonging to one of these classes (and choosing the appropriate fixation material) when the condylar fracture is bilateral. It is worth exploring the significant and strong relation between CSI and the base of the condyle (width or thickness), where fracture of the processus condylaris usually does not reach. Measurements of the unaffected condylar base are easy to obtain in most cases due to its characteristic localization at the same level as the sigmoid notch, even if the condylar fracture is displaced (Kozakiewicz, 2019).

The proposed clinico-anatomical classification method avoids the problems associated with incorrect plate selection (Fig. 7). Group assignments can be made by making one measurement (Width_neck_basal). Thus, the surgeon is able to select the optimal fixation material before the surgery begins with great intraoperation time savings (Fig. 8).

Exceptions include patients with a Width_neck_basal measurement in the range of 8.5–11.5 mm, for which additional measurements must be made. Another issue is fracture of the condylar base or the ramus of the mandible, as the fracture line ruptures the condylar base. If the fracture line is below the point of Width_neck_basal measurement, then slender/squat classification is still possible. In addition, all condylar neck fractures, both low and high, can still be evaluated by the proposed method. The required fixation material can be chosen before surgery commences.

A final outcome of this original study is the identification of a link between anatomy and clinical anatomy for maxillofacial surgeons. This study can also be beneficial for practical teachings of anatomy among dental faculty students.

5. Conclusion

In conclusion, the classification of mandibular condyle posture into slender and squat types is possible based on the radiological anatomy and can be useful in choosing the most appropriate fixation material choice in maxillofacial traumatology.

Ethical statement

The approval of the bioethics committee number: RNN/125/15/KE and RNN/738/12/KB were obtained for the study.

Declaration of interest

Both authors must disclose any financial and personal relationships with other people or organizations that could inappropriately influence (bias) their work.

Funding statement

This study was supported by Medical University of Lodz grant No. 503/5-061-02/503-51-001 and 503/5-061-02/503-51-002.

Ethical statement

The approval of the bioethics committee number: RNN/125/15/KE and RNN/738/12/KB were obtained for the study.

Declaration of interest

Both authors must disclose any financial and personal relationships with other people or organizations that could inappropriately influence (bias) their work.

CRediT authorship contribution statement

Bartosz Bielecki-Kowalski: Data curation, Formal analysis, Investigation, Project administration, Visualization, Writing - original draft, Writing - review & editing. **Marcin Kozakiewicz:** Conceptualization, Formal analysis, Funding acquisition, Methodology, Project administration, Supervision, Validation, Writing - review & editing.

Appendix A. Supplementary data

Supplementary material related to this article can be found, in the online version, at doi:https://doi.org/10.1016/j.aanat.2020.151616.

References

Al-Moraissi, E.A., Louvrier, A., Colletti, G., Wolford, L.M., Biglioli, F., Ragaey, M., Meyer, C., Ellis, E., 2018. Does the surgical approach for treating mandibular condylar fractures affect the rate of seventh cranial nerve injuries? A systematic review and meta-analysis based on a new classification for surgical approaches. J. Cranio-maxillofacial Surg. 46 (3), 398–412, http://dx.doi.org/10.1016/j.jcms.2017.10.024.

Aquilina, P., Chamoli, U., Parr, W.C.H., Clausen, P.D., Wroe, S., 2013. Finite element analysis of three patterns of internal fixation of fractures of the mandibular condyle. Br. J. Oral Maxillofac. Surg. 51, 326–331, http://dx.doi.org/10.1016/j.bjoms.2012.08.007.

Asprino, L., Consani, S., 2006. A Comparative Biomechanical Evaluation of Mandibular Condyle Fracture. J. Oral Maxillofac. Surg. 64, 452–456, http://dx.doi.org/10.1016/j.joms.2005.11.017.

Baillard, C., Barillot, C., 2000. Robust 3D segmentation of anatomical structures with level sets. In: Delp, S.L., DiGoia, A.M., Jaramaz, B. (Eds.), Medical Image Computing and Computer-Assisted Intervention – MICCAI 2000. MICCAI 2000. Lecture Notes in Computer Science, vol 1935. Springer, Berlin, Heidelberg, pp. 236–245, http://dx.doi.org/10.1007/978-3-540-40899-4_24.

Bataineh, A.B., 1998. Etiology and incidence of maxillofacial fractures in the north of Jordan. Oral Surg. Oral Med. Oral Pathol. Oral Radiol. Endod. 86 (1), 31–35, http://dx.doi.org/10.1016/S1079-2104(98)90146-9.

Bhutia, O., Kumar, L., Jose, A., Roychoudhury, A., Trikha, A., 2013. Evaluation of facial nerve following open reduction and internal fixation of subcondylar fracture through retromandibular transparotid approach. Br. J. Oral Maxillofac. Surg. 52, 236–240, http://dx.doi.org/10.1016/j.bjoms.2013.12.002.

Brasileiro, B.F., Passeri, L.A., 2006. Epidemiological analysis of maxillofacial fractures in Brazil: a 5-year prospective study. Oral Surgery, Oral Medicine, Oral Pathology, Oral Radiology and Endodontology 102 (1), 28–34, http://dx.doi.org/10.1016/j.tripleo.2005.07.023.

Brin, I., Jarjoura, R., Regev, E., 2012. Morphological occlusal features following condylar fractures in children. Eur. J. Orthod. 34, 147–151, http://dx.doi.org/10.1093/ejo/cjq154.

Bruneau, S., Courvoisier, D.S., Scolozzi, P., 2018. Facial Nerve Injury and Other Complications Following Retromandibular Subparotid Approach for the Management of Condylar Fractures. J. Oral Maxillofac. Surg. 76 (4), 812–818, http://dx.doi.org/10.1016/j.joms.2017.11.003.

Cascone, P., Spallaccia, F., Maria, F., Fatone, G., Rivaroli, A., Iannetti, G., 2008. Rigid versus semirigid fixation for condylar fracture : experience with the external fixation system. J. Oral Maxillofac. Surg. 66, 265–271, http://dx.doi.org/10.1016/j.joms.2007.06.621.

Chrcanovic, B.R., Freire-Maia, B., Souza, L.N.de, Araújo, V.O.de, Abreu, M.H., 2004. Facial fractures: a 1-year retrospective study in a hospital in Belo Horizonte. Pesquisa Odontológica Brasileira = Brazilian Oral Research 18 (4), 322–328, http://dx.doi.org/10.1590/s1806-83242004000400009.

Ellis, E., McFadden, D., Simon, P., Throckmorton, G., 2000. Surgical complications with open treatment of mandibular condylar process fractures. J. Oral Maxillofac. Surg. 58 (9), 950–958, http://dx.doi.org/10.1053/joms.2000.8734.

Ellis, E., McFadden, D., Simon, P., Throckmorton, G., 2009. Treatment of mandibular condylar process fractures. J. Oral Maxillofac. Surg. 58, 950–958, http://dx.doi.org/10.1053/joms.2000.8734.

Juniper, R.P., 1994. The shape of the condyle and position of the meniscus in temporomandibular joint dysfunction. Brit J Oral Max Surg. 32, 71–76, http://dx.doi.org/10.1016/0266-4356(94)90130-9.

Korzon, T., Kruk, J., 1971. Ocena odległych wyników zachowawczego leczenia złamań wyrostka kłykciowego żuchwy. Czas Stomat 24, 157–161.

Kozakiewicz, M., 2019. Classification proposal for fractures of the processus condylaris mandibulae. Clin. Oral Investig. 23, 485–491, http://dx.doi.org/10.1007/s00784-018-2459-1.

Kozakiewicz, M., Swiniarski, J., 2013. "A" shape plate for open rigid internal fi xation of mandible condyle neck fracture. J. Craniomaxillofac. Surg. 5, 1–8, http://dx.doi.org/10.1016/j.jcms.2013.11.003.

Kozakiewicz, M., Świniarski, J., 2017. Treatment of high fracture of the neck of the mandibular condylar process by rigid fixation performed by lag screws : finite element analysis Leczenie wysokiego złamania szyjki wyrostka kłykciowego żuchwy poprzez sztywne unieruchomienie śrubami – analiza z wykorzystaniem elementów skończonych. Dent. Med. Probl. 54, 223–228, http://dx.doi.org/10.17219/dmp/75907.

Meyer, C., Kahn, J.L., Boutemi, P., Wilk, A., 2002. Photoelastic analysis of bone deformation in the region of the mandibular condyle during mastication. J. Craniomaxillofac. Surg. 30 (3), 160–169.

Neff, A., Cornelius, C.P., Rasse, M., Torre, D.D., Audigé, L., 2014. The comprehensive AOCMF classification system: condylar process fractures - Level 3 tutorial. Craniomaxillofacial Trauma Reconstr. Open 7, 44–58, http://dx.doi.org/10.1055/s-0034-1389559.

Newhauser, W., Jones, T., Swerdloff, S., Newhauser, W., Cilia, M., Carver, R., Halloran, A., Zhang, R., 2014. Anonymization of DICOM electronic medical records for radiation therapy. Comput. Biol. Med. 53, 134–140.

Rajchel, J., Ellis, E., Fonseca, R.J., 1986. The anatomical location of the mandibular canal: its relationship to the sagittal ramus osteotomy. Int. J. Adult Orthodontics Orthognathic Surg. 1 (1), 37–47.

Silvennoinen, U., Iizuka, T.L.C., 1992. Different patterns of condylar fractures: an analysis of 382 patients in a 3-year period. J. Oral Maxillofac. Surg. 50 (1032).

Wagner, A., Krach, W., Schicho, K., Undt, G., Ploder, O., Ewers, R., 2002. A 3-dimensional finite-element analysis investigating the biomechanical behavior of the mandible and plate osteosynthesis in cases of fractures of the condylar process. Oral Surg. Oral Med. Oral Pathol. Oral Radiol. Endod. 94, 678–686.

Yale, S.H., Ceballos, M., Kresnoff, C.S., Hauptfuehrer, J.D., 1963. Some observations on the classification of mandibular condyle types. Oral Surgery, Oral Surg Oral Med Oral Pathol. 16, 572–577, http://dx.doi.org/10.1016/0030-4220(63)90146-4.